Hindawi
Geofluids
Volume 2021, Article ID 5583877, 15 pages
https://doi.org/10.1155/2021/5583877

Research Article

Analysis of Mining Crack Evolution in Deep Floor Rock Mass with Fault

Juntao Chen,[1,2,3] Yi Zhang,[1] Kai Ma,[4] Daozeng Tang,[1] Hao Li,[1] and Chengxiang Zhang[5]

[1]*College of Mining and Safety Engineering, Shandong University of Science and Technology, Qingdao 266590, China*
[2]*College of Geosciences and Surveying Engineering, China University of Mining and Technology, Beijing 100083, China*
[3]*Shandong Energy Linyi Mining Group Co., Dezhou, Shandong 251105, China*
[4]*School of Resources and Civil Engineering, Northeastern University, Shenyang 110819, China*
[5]*Shandong Energy Zibo Mining Group Co., Ltd, Zibo, Shandong 255100, China*

Correspondence should be addressed to Kai Ma; 1208988922@qq.com and Daozeng Tang; 2380109630@qq.com

Received 28 January 2021; Accepted 7 October 2021; Published 3 December 2021

Academic Editor: Dan Ma

To further explore the crack evolution of floor rock mass, the mechanism of fault activation, and water inrush, this paper analyzes the crack initiation and propagation mechanism of floor rock mass and obtains the initiation criteria of shear cracks, layered cracks, and vertical tension cracks. With the help of simulation software, the process of fault activation and crack evolution under different fault drop and dip angles was studied. The results show that the sequence of crack presented in the mining rock mass is vertical tension cracks, shear cracks, and layered cracks. The initiation and propagation of the shear cracks at the coal wall promote the fault activation, which tends to be easily caused at a specific inclination angle between 45° and 75°. The fault drop has no obvious impact on the evolution of floor rock cracks and will not induce fault activation. However, the increase of the drop will cause the roof to collapse, reducing the possibility of water inrush disaster. Research shows that measures such as adopting improved mining technology, reducing mining disturbance, increasing coal pillar size, and grouting before mining as reinforcement and artificial forced roof can effectively prevent water inrush disasters caused by deep mining due to fault activation.

1. Introduction

Mine water disaster is an important factor threatening the safety in coal mining and is only after gas outburst as the dangerous factor to mining whereas the water inrush disaster is particularly outstanding in the deep mining with high confined water. The field measurement of water inrush shows that most of water inrush accidents in deep mining are caused by the conduction of primary channels with delays of different time spans [1, 2], while water inrush due to fault activation is more common [3]. Water inrush induced by fault activation means that the fault does not conduct water in the initial state, but under the action of mining disturbance, in situ stress, confined water, and other factors, the fault structure is dislocated and activated to conduct aquifer and induce water inrush [4, 5]. The research shows that the evolution from crack of floor rock mass to water inrush due to fault activation is a process from quantitative change to qualitative change [6]. Therefore, study on the crack evolution from quantitative change to qualitative change in floor mining rock mass is of great significance for prevention of water inrush caused by fault activation [7, 8].

With increasing mining depth, the gap between the coal-mining seam and the Ordovician thick limestone is getting closer with some of the water pressure exceeding 20 MPa, increasing the possibility of fault activation conducting aquifers to induce water inrush disasters. At the same time, the deep complex environment makes the expansion of rock cracks more irregular [9–11]. In recent years, scholars have conducted laboratory experiments [12–18], theoretical analysis [19–21], numerical calculations [22–24], and field measurements [25–27] on fault water inrush mechanism, time-dependent characteristics, and risk

assessment methods. Numerous achievements have been achieved such as quantitatively deriving the water inrush issue from faults based on mechanics and mathematics, thus obtaining the criteria for the occurrence of water inrush from the floor under different conditions [2, 28–30]; in terms of numerical calculations, structural analysis has conducted to study fault activation with water seepage by FLAC3D. It is proved that COMSOL Multiphysics shows high applicability for the fluid-solid coupling problem of floor fault water inrush with promising application; in terms of field measurement, the field water detection and release equipment and the research and development of key governance technologies were strengthened to achieve a high-precision description of the development of rock mass fissures, which is of great significance for evaluating the risk of water inrush.

Nowadays, most scholars have studied the water inrush hazards with fault from a macro perspective, ignoring the essential impact of crack evolution on fault activation. However, the fault activation and water inrush are the result of quantitative changes in microscopic crack evolution in rock mass. To this end, this paper takes the perspective of deep rock mass crack evolution with fault, explores the evolution characteristics of deep floor, and obtains the initiation and expansion criteria for different cracks in the seam floor; the mining simulation is carried out on the floor with fault to analyze the influence of fault dip and drop on the rock mass crack evolution and fault activation. At the same time, relevant measures to prevent fault activation and water inrush disasters are also proposed.

2. Criterion Analysis of Crack Initiation of Floor Rock Mass with Faults

The cracks in the mining rock mass are mainly formed under the tensile shear and compression shear. Based on the "Three-zones" Theory [31, 32] and according to the formation mechanism and location of the cracks, this paper divides the floor rock mass crack into shear crack, stratified crack, and vertical tension crack [8]. The following offer respective analysis on the initial cracking criterion of the three types of mining rock fractures.

2.1. Initial Cracking Criterion of Shear Fracture. Assuming that the floor rock mass develops any weak fracture surface ab, the angle between the outer normal line n and the horizontal direction is α, and it is affected by the principal stress σ_1, σ_3, and the seepage pressure P. If there is no seepage pressure, then P is 0.

According to the Mohr-Coulomb strength criterion, if the normal stress σ_α and shear stress τ_α were imposed on the fracture surface of the rock, then its shear strength would be:

$$\tau = c + \sigma \tan \varphi, \tag{1}$$

where c is the bonding force of the crack surface and φ is the internal friction angle of the crack surface.

The analysis shows that effective stress on the crack surface is $\tau' = \tau_\alpha - (c + \sigma_\alpha \tan \varphi)$. If $\tau' > 0$, the shear cracks in the seam floor rock mass will initiate cracking, namely:

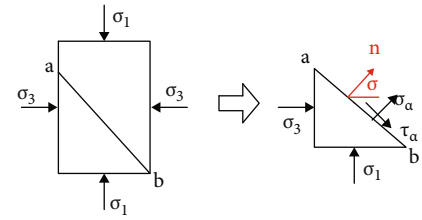

Figure 1: Stress state of fracture surface of floor.

$$\sigma_1 > \frac{(\sin 2\alpha - \cos 2\alpha \tan \varphi - \tan \varphi)\sigma_3 - 2P \tan \varphi + 2c}{\sin 2\alpha - \cos 2\alpha \tan \varphi + \tan \varphi}. \tag{2}$$

When σ_1 and σ_3 are imposed on the fracture and P is qualified for formula (2), the rock mass shear fracture will crack. Therefore, formula (2) is the initiation criterion of the shear fracture of the rock mass containing the fault floor. The initiation of the fissure promotes the formation of the water channel as the initiation direction is generally at a certain angle with the horizontal rock formation; it will change the path of the confined water leading up the working surface along the fissure.

2.2. Criterion of Initiation of Layered Cracks. The floor rock mass will undergo different degrees of bending deformation under high stress, high confined water, and strong mining disturbances, resulting in the formation of normal opening and horizontal shear layered cracks between rock layers. Once the fault is activated, water channel is highly easy to be formed in the weak areas of fissures, creating the space for the high-pressure aquifer to flow into the stope or goaf.

2.2.1. Normally Opening Layered Cracks. Normally opening layered cracks is mainly caused by the repeated compression-expansion-compression of the seam floor rock mass after coal seam mining and the difference in rock properties, as shown in Figures 1 and 2. Under stress, when the flexural rigidity of the upper rock layer of the curved rock mass is smaller than the flexural rigidity of the lower rock layer, a normal opening layer crack will occur between the upper and lower rock layers. The horizontal component σ_h and vertical component σ_v of ground stress follow the Ginnick hypothesis, and the horizontal component of ground stress is dominated by compression stress, and the degree of bending of the seam floor rock can be expressed as:

$$K = \frac{\sigma_{h1}}{\delta} = \frac{\sigma_h \sin \beta}{\delta} = \frac{\mu \sigma_v \sin \beta}{(1-\mu)\delta} = \frac{\mu \gamma z \sin \beta}{(1-\mu)\delta}. \tag{3}$$

Therefore

$$\delta = \frac{\mu \gamma z \sin \beta}{(1-\mu)K}, \tag{4}$$

where K is the stiffness index of the rock formation, σ_{h1} is the stress of σ_h perpendicular to the direction of the curved rock face, β is the angle between the tangent of the curved rock

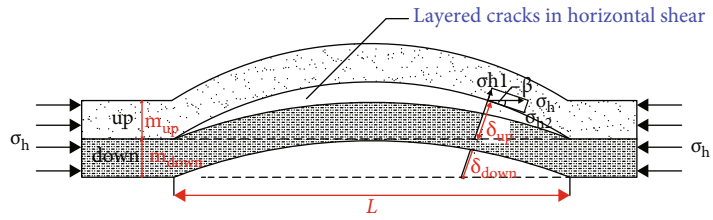

Figure 2: Sketch map of normal opening layer to fissure formation.

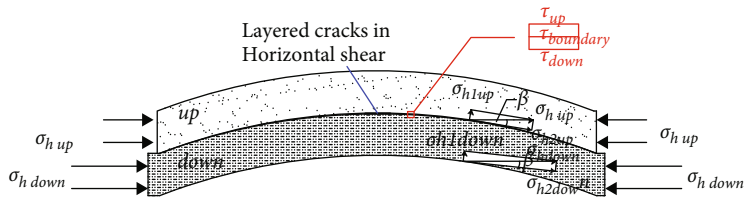

Figure 3: Sketch of formation of horizontal shear layer to fissure.

face and the horizontal plane, μ is the Poisson's ratio of the rock formation, δ is the bending displacement of the rock formation under σ_{h1}, γ is the bulk density of the floor rock, and z is the buried depth of the floor, as shown in Figure 2.

It can be seen from equation (4) that when the same rock layer is bent under external force (where μ, γ, z, and K have the same values), the higher the β, the higher the δ and the more likely the rock layer will be bent and deformed. β reaches its biggest value at both ends of the bottom curved rock layer and drops to 0 at the top of the curved surface, indicating that during the coal mining process, the continuous bending of the bottom rock layer starts from both ends of the rock layer, not the top. It can be seen from equation (3) that when the stiffness of the upper rock layer is weaker than that of the lower rock layer ($K_{\text{upper}} < K_{\text{lower}}$, then the stresses on the upper and lower adjacent rock layers are approximately equal at this time), the bending displacement of the upper rock layer is greater than the bending displacement of the lower rock layer ($\Delta_{\text{up}} > \delta_{\text{down}}$). At this time, the upper and lower strata will have normal opening and stratification cracks, and the expression of the bending displacement of the strata is

$$\delta = \omega_{\max} = \varepsilon \frac{\gamma_1 L^4}{32Em^2}, \tag{5}$$

where $\omega_{\max}$ is the maximum deflection of the floor rock and ε is the determination coefficient of the beam support conditions. The fixed beam is 1, and the simply supported beam is 5; γ_1 is the bulk density of the floor rock; L is the bending span of the floor rock; E is the elastic modulus of the floor rock (the upper and lower ones are expressed as E_{upper} and E_{lower}, respectively); m is the thickness of the floor rock layer (the upper and lower rock layers are expressed as m_{upper} and m_{lower}, respectively).

It can be seen from equation (5) that, without considering the difference in bulk density of adjacent rock formations on the floor, if $\delta_{\text{up}} > \delta_{\text{down}}$, then $E_{\text{up}}m_{\text{up}}^2 < E_{\text{down}}m_{\text{down}}^2$. Therefore, the conditions for the generation of the cracks in the normal expansion layer are $E_{\text{up}}m_{\text{up}}^2 < E_{\text{down}}m_{\text{down}}^2$. The generation of this type of cracks is related to the elastic modulus and thickness of the upper and lower adjacent rock layers. The greater the difference between the product of the upper and lower rock layers' elastic modulus and the square of the thickness, the more conducive to the formation of normal open cracks. From the actual situation of the site, the conditions for the formation of cracks in normal opening layers are relatively easy to achieve, so fault cracks are very easy to develop and expand between rock layers.

2.2.2. Layered Cracks in Horizontal Shear. According to the literature [32], when the shear stress at the interface of adjacent floor rocks is greater than its maximum allowable shear stress, shear slip will occur at the interface of the rock formations, resulting in horizontal shear fissures. Compared to normal opening layers, this crack has a smaller opening. If the shear stress difference in the thickness direction of a certain floor rock layer is neglected, the shear stress of the rock layer on the layer section can be approximated as the tangential stress σ_{h2} of σ_h. The shear stress on the section of adjacent upper and lower strata can be approximated by the following formula:

$$\begin{cases} \tau_{\text{up}} \approx \sigma_{h2\,\text{up}} = \sigma_{h1\,\text{up}} \cos\beta, \\ \tau_{\text{down}} \approx \sigma_{h2\,\text{down}} = \sigma_{h1\,\text{down}} \cos\beta, \end{cases} \tag{6}$$

where τ up and τ down are the shear stresses of the upper and lower strata in any upper or bottom layer, $\sigma_{h\,\text{up}}$ and $\sigma_{h\,\text{down}}$ are the horizontal components of the ground stress on the upper and lower strata, respectively, and $\sigma_{h2\,\text{up}}$ and $\sigma_{h2\,\text{down}}$ are the tangential stresses of the horizontal components of the ground stress on the upper and lower strata, respectively, as shown in Figure 3.

The shear stress τ boundary at the interface of adjacent rock formations is not equal to the shear stress of the upper and lower rock formations on the layer-direction

section. Take a tiny element on the interface, as shown in Figure 3, and with the physical equation of elasticity, we could get [33]:

$$\begin{cases} \gamma_{\text{up}} = \dfrac{2\left(1+\mu_{\text{up}}\right)}{E_{\text{up}}}\tau_{\text{up}}, \\ \gamma_{\text{down}} = \dfrac{2(1+\mu_{\text{down}})}{E_{\text{down}}}\tau_{\text{down}}, \\ \gamma_{\text{boundary}} = \dfrac{2\left(1+\mu_{\text{boundary}}\right)}{E_{\text{boundary}}}\tau_{\text{boundary}}, \end{cases} \tag{7}$$

where γ_{up}, γ_{down}, and γ_{boundary} are the shear strains of the upper and lower strata section and the interface, respectively, γ_{up}, γ_{down}, and γ_{boundary} are the Poisson's ratios of the upper and lower strata section and the rock mass at the interface, respectively, E_{boundary} is the rock masses at the interface and the modulus of elasticity, and τ_{boundary} is the shear stress at the interface.

Since the unit body taken is small, the size can be represented by the absolute value of the difference between and

$$\left|\gamma_{\text{boundary}}\right| = \left|\gamma_{\text{up}} - \gamma_{\text{down}}\right|. \tag{8}$$

Substituting equations (6) and (8) into equation (7), the shear stress $|\tau_{\text{boundary}}|$ at the interface of adjacent rock formations can be obtained as:

$$\left|\gamma_{\text{boundary}}\right| = \frac{\left|\left(2\left(1+\mu_{\text{up}}\right)/E_{\text{up}}\right)\sigma_{h\,\text{up}} - (2(1+\mu_{\text{down}})/E_{\text{down}})\sigma_{h\,\text{down}}\right|E_{\text{boundary}}\,cos\beta}{2\left(1+\mu_{\text{boundary}}\right)} = \left|\frac{\sigma_{h\,\text{up}}}{G_{\text{up}}} - \frac{\sigma_{h\,\text{down}}}{G_{\text{down}}}\right|G_{\text{boundary}}cos\beta = \left|\gamma_{\text{boundary}}\right|G_{\text{boundary}}, \tag{9}$$

where G_{up}, G_{down}, and G_{boundary} are the shear modulus of the upper and lower rock formations and their interfaces, respectively.

Suppose the ultimate shear stress of the rock interface is $[\tau_{\text{boundary}}]$, when $|\tau_{\text{boundary}}|$ is bigger than $[\tau_{\text{boundary}}]$, shear slip will happen in the adjacent rock layers, forming a shear layered crack. It can be seen from equation (9) that the bigger the difference between the ratio of the horizontal stress and the shear modulus of the upper and lower rock formations and the shear modulus at the interface, the more likely the adjacent rock formations are to undergo shear slippage to form a shear layered crack. In addition, β angles at both ends of the curved rock layer are the largest, and the top of the middle of the curved surface is 0. Under certain conditions of other influencing factors, the shear stress at the interface between the two ends of the curved floor rock is smaller than that on the top of the curved rock layer, indicating that at the end and top interface, shear slip is most likely to occur and form horizontal shear layer cracks after coal mining, which requires special attention.

2.3. Vertical Tension Crack Initiation Criterion. Vertical tension cracks are caused by the bending stress of the floor rock mass that exceeds the tensile strength of the rock under the combination of horizontal compression stress and confined water. Cracks usually appear in the middle section of the curved rock, as shown in Figure 4. When rock's tensile stress $\sigma_{x\,\text{total}} > [\sigma_s]$, a vertical tensile crack appears [21], and $[\sigma_s]$ is the ultimate tensile strength of the floor rock.

Vertical tension cracks will induce vertical rising of pressurized water along the crack surface, and the stress acting on the crack surface is in the same direction as the bending stress received by the crack, which further promotes the opening of the crack surface and accelerates the formation of the water channel on vertical evolution of the crack.

3. Analysis of Mining Crack Propagation in Floor Rock Mass

3.1. Crack Propagation in Mining Rock Mass. According to fracture mechanics, the rock mass fissures are divided into types I, II and III. When the stress field at the crack tip is constant, the strength of the tip crack is completely determined by the stress intensity factor. If the stress intensity factor of a rock mass crack is greater than its fracture toughness, the crack will expand forward.

Fault activation causes the confined water to flow up along the fractured zone of the fault, and the fractures in some rock masses are filled with confined water, which mainly exists on the surface of the fracture in the form of hydrostatic pressure. At this time, the stress intensity factor at the tip of the rock mass fracture is

$$K_{(P)} = \alpha_I P\sqrt{\pi a}, \tag{10}$$

where α_I is the geometrical factor of type I fracture and a is the length of the major axis of the fracture.

For the fractures filled by confined water, the fracture surface is stretched outward by the confined water. Therefore, the stress intensity factor at the tip of a water-filled fracture near the fracture zone should be:

$$K_{I\,\text{sum}} = K_I + K_{(P)}, \tag{11}$$

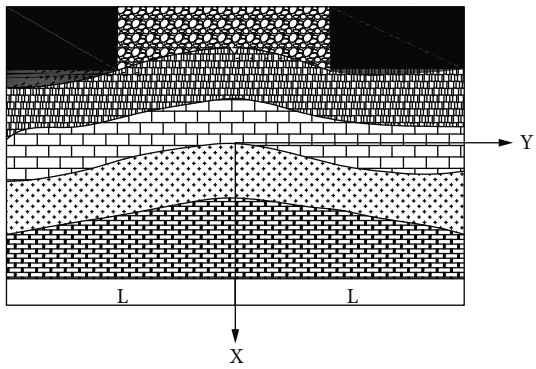

Figure 4: Formation of vertical tension crack.

where K_I is the stress intensity factor of type I (open crack).

In the formation of the water channel in the seam floor with faults, there are three main types of crack propagation in rock mass: (1) the tip of the crack with propagation between unfilled cracks is mainly affected by the mining disturbance with no hydraulic pressure; (2) the propagation of water-filled fissures and non-water-filled fissures mostly occurs at the confined water rise top interface, the water flow top interface of the fault water conduction fracture zone, and the tip of the rock mass water-filled fissure; and (3) the propagation and penetration between the water-filled cracks are mainly affected by water pressure and mining disturbances and mostly occur in the water-filled area of the fracture after the confined water is lifted, which is conducive to the mutual penetration and outward propagation of the water-filled fractures, as shown in Figure 5.

3.2. Mining Rock Crack Propagation Criterion. If the influence of water filling of rock mass cracks is not considered, the circumferential stress at the tip of type I and type II cracks [30]:

$$\sigma_\theta = \frac{1}{\sqrt{2\pi r}} \cos\frac{\theta}{2}\left[\frac{K_I}{2}(1+cos\theta) - \frac{3K_{II}}{2}\sin\theta\right], \quad (12)$$

where (r, θ) is the local polar coordinate with the crack tip as the origin.

According to the theory of maximum circumferential stress, the angle θ_0 of the crack propagation direction of rock mass should satisfy:

$$\left.\frac{\partial\sigma_\theta}{\partial\theta}\right|_{\theta=\theta_0} = 0, \left.\frac{\partial^2\sigma_\theta}{\partial\theta}\right|_{\theta=\theta_0} < 0. \quad (13)$$

Therefore, when $\theta \in [0, \pi/2]$, $\cos(\theta/2) \neq 0$, the following equation is sure to happen:

$$K_I \sin\theta_0 + K_{II}(3\cos\theta_0 - 1) = 0. \quad (14)$$

And then

$$\theta_0 = arc\cos\frac{3K_{II}^2 \pm \sqrt{K_I^2 + 8K_I^2K_{II}^2}}{K_I^2 + 9K_{II}^2}. \quad (15)$$

According to formula (15), the rock fracture will expand along the θ_0 direction. When $\theta = \theta_0$, the circumferential stress of the crack reaches the maximum

$$\sigma_{\theta_{max}} = \sigma_\theta(r_0, \theta_0) = \frac{1}{\sqrt{2\pi r_0}} \cos\frac{\theta_0}{2}\left[\frac{K_I}{2}(1+\cos\theta_0) - \frac{3K_{II}}{2}\sin\theta_0\right]. \quad (16)$$

Therefore, when $\sigma_{\theta\,\max} = \sigma_{\theta c}$ ($\sigma_{\theta c}$ is the ultimate stress for crack propagation), the fracture of rock mass containing faults will expand along the θ_0 direction; that is, the criterion for the propagation of rock mass cracks is

$$K_{Ic} = \cos\frac{\theta_0}{2}\left(K_I\cos^2\frac{\theta_0}{2} - \frac{3K_{II}}{2}\sin\theta_0\right). \quad (17)$$

It can be seen from equation (17) that the continuous propagation of rock mass cracks in the fault floor is related to the stress intensity factor and the crack dip angle of the rock mass cracks. The larger the stress intensity factor, the closer that crack dip angle to θ_0 and the easier for rock mass cracks to propagate. According to equation (17), three methods are proposed to prevent the cracks in the fault-bearing rock mass from propagating and forming water channels:

(1) Improve the coal mining method and mining technology in the working face, reduce the force of the supporting pressure on the fault surrounding rock and the seam floor, reduce the stress intensity factor of the fault surrounding rock and floor rock mass cracks, such as backfill mining, etc.

(2) Dynamic monitoring of the fracture development of the fault-bearing rock mass should be carried out in time to avoid the inclination of the mining rock mass fracture approaching to θ_0

(3) Improve the strength of the fault rupture zone and those weak zones and reduce the possibility of water inrush caused by the crack propagation by increasing the fracture toughness of the mining rock mass fracture, such as grouting on the fault rupture zone and surrounding rock before coal mining

4. Simulation Analysis of Crack Evolution of in Floor Rock Mass

In order to reveal the law of evolution of fractures in rock mass in seam floor with fault and to explore the influence of fault occurrence on the development process and activation of fractures in floor rock masses, the paper used the RFPA software to simulation the evolution process of fractures in rock mass in seam floor with fault.

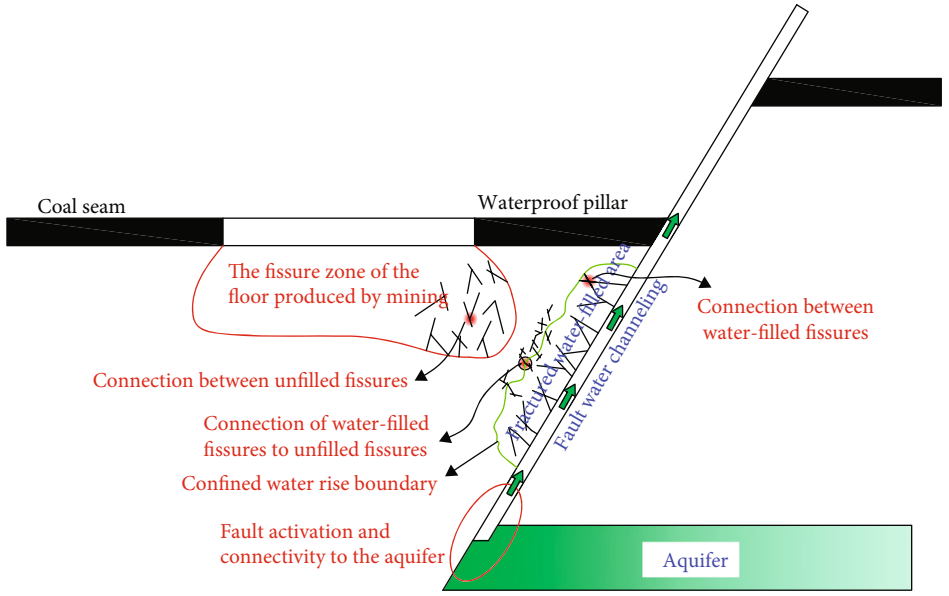

Figure 5: Crack propagation in rock mass with fault.

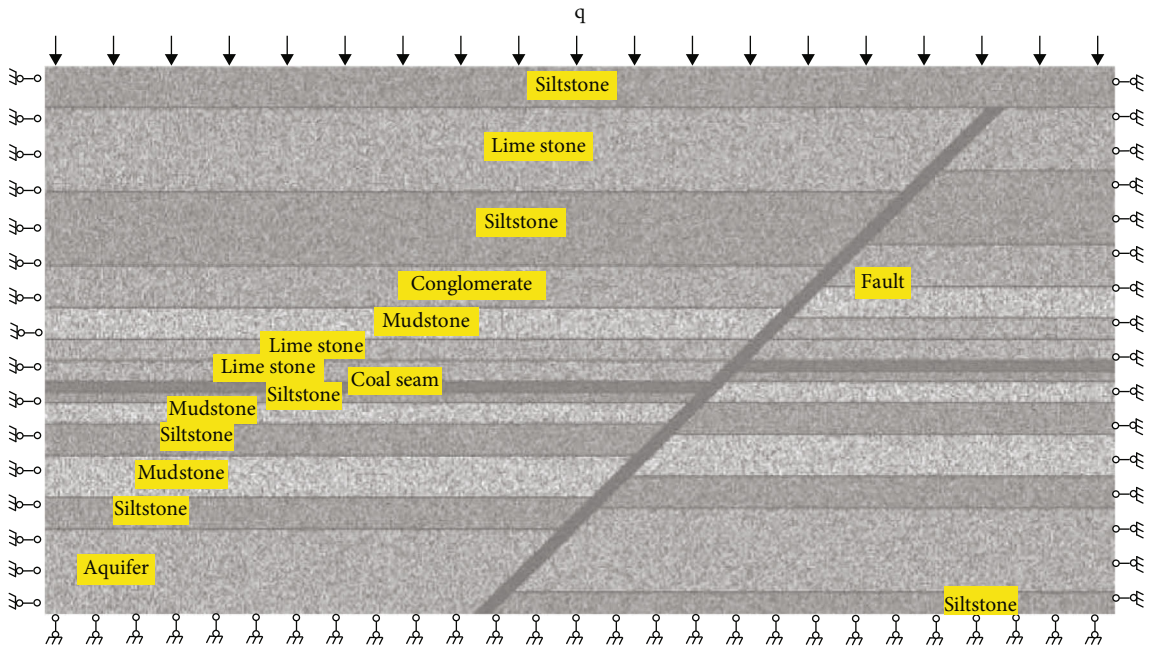

Figure 6: Numerical calculation model of deep mining with fault.

4.1. Establish the Model. Based on the hydrogeological characteristics of the water-bursting mine in the Jibei mining area, Shandong Province, China, a model for the crack evolution is designed, as shown in Figure 6. The model is divided into $500 \times 260 = 130000$ equal area units. Equivalent uniform load is applied to the top of the model with 4 MPa water pressure transmitted to the aquifer through the boundary. The conditions for the boundaries of the model are as follows: the left and right boundaries are horizontally constrained and movable vertically and fixed bottom, and the top and bottom ends are water-proof boundaries. The simulation is solved according to the stationary problem, and the plane-strain model is used to analyze the evolution process of the cracks in the mining rock mass of the floor.

The simulated design coal seam mining thickness is 5 m with mining the full height at one time and advancing step by step as main mining method. The coal seam is excavated from left to right. The cut hole is 110 m away from the left boundary of the model, and 60 m of fault-proof coal pillars is reserved. The excavation step is 5 m. Fault dip and drop

are important parameters for water inrush disasters which have been extensively researched by scholars [33]. In order to further clarify the influence of fault drop and dip on fault activation and water inrush and verify the accuracy of the rock crack evolution criterion, this paper designs five sets of simulation schemes with different fault dips and dips, as shown in Table 1.

Table 1: Simulation design schemes.

Project	Buried depth H/m	Fault dip α_f/°	Fault drop h/m	Hydraulic pressure P/MPa
1	1000	45	10	4
2	1000	60	10	4
3	1000	75	10	4
4	1000	45	30	4
5	1000	45	50	4

4.2. Simulation Result Analysis Overlying Strata Separate Appear

4.2.1. The Influence of Different Fault Dips on the Evolution of Fractures in the Mining Rock Mass with Fault. (a)–(d) in Figures 7–9 are diagrams of the evolution state of the cracks in the floor rock mass with the fault dip angles of 45°, 60°, and 75° when the working face advances. During the on-site coal seam mining process, floor water inrush often occurs on the eve of the initial fracture of the basic roof, and the collapse of the basic roof can restrain the further destruction of the floor rock mass and slow down the formation of water channels. Therefore, in the process of coal seam advancement, the break of the roof is the final simulation state.

It can be seen from Figures 7–9 that when the working face is advanced by 50 m, the supporting pressure of the overburden rock acts on the coal and rock mass in front of the working face, resulting in greater stress concentration. Vertical tension cracks appear in the floor when the floor is damaged. As the working face continues to advance to 75 m, shear cracks appear at the junction of the coal wall and the floor. At the same time, floor is being further damaged. Vertical tension cracks extend deeper, and some minor number of layered cracks are produced at 75° fault dip. As shown in Figure 9(b) when the working face advances to 105 m, the shear fissure at the coal wall expands to the fault zone, forming a weak area, and the fault zone is disturbed but not activated. Layered cracks in the floor continued to evolve whereas the vertical tension cracks mainly develop in depth, ending up with crack propagation and penetration gradually, as shown in Figure 8(c). When the working face advances to 140 m, the shear fissure at the coal wall further evolves into the fault zone. The roof collapses show up for the first time, and the shear fissure in the weak area of the coal wall further expands to the fault zone, but cracks under the goaf will stop expanding to the depth, as shown in Figure 9(d). When the dip angle of fault is 60°, cracks initially appear and then develop toward the fault along with the process of compression-expansion-compression. These cracks, such as shear crack, layer crack, and tensile crack propagate and coalesce, forming the water inrush channels from goaf to fault. Besides, due to the concentration stress loaded on the fault safely pillar, which produce great tensile stress on the overlying strata, and shear stress along the fault plane, which is induced by compression, the fault slips, and activate gradually is presented with the increase of two stress above.

The analysis shows that cracks in the coal floor rock with fault locate in different positions. In the seam floor, the vertical tension cracks are mainly developed in depth with little impact on water inrush when special structures do not exit. Layered cracks are more difficult to form and not easy to propagate. But once formed, they usually have a greater impact on the formation of fault water channels. At the junction of coal walls and the floor, the shear fissures are mainly developed towards the fault zone, coupling with layered fissures, thus accelerating the formation of fault water channels.

Further comparative analysis of the crack evolution process of coal floor rock with fault in Figures 7–9 shows that when the working face advances to 140 m, only the fault with a dip of 60° is activated, and the shear fracture propagation speed and extent at the coal wall are the strongest, accompanied by crack penetration, as shown in Figure 8(d). This indicates that there is a specific dip in the range of 45°~75°making the fault easier to activate. This is consistent with previous conclusion that "the dip is at the adjacent value of θ_0, and the fault fracture zone is prone to activation." However, the relationship between the dip angle of the particular fault and θ_0 still needs to be further studied.

4.2.2. The Influence of Different Fault Drop on the Fracture Evolution of Coal Floor Rock with Fault. The (a)–(d) in Figures 7, 10, and 11 are diagrams of the evolution of the cracks in the coal floor rock with fault with the fault drop of 10 m, 30 m, and 50 m when the working face advances forward. In the simulation test, when the fault drop was 50 m, the roof broke for the first time when the mining reached 105 m. Therefore, there is no diagram when the working face advances to 140 m in Figure 11. Figure 11 (c1 and c2) shows the intermediate change state and final state when the working face advances 105 m (the middle step of the simulation step is different).

It can be seen from Figures 7, 10, and 11 that under different fault drops, the initiation and propagation evolution of the floor rock mass cracks are roughly the same as those in Figures 8 and 9 as the working face advances. This indicates that the fault drop has little influence on the floor rock mass crack evolution, and the fault has not been activated throughout the simulation process. In addition, as the fault drop increases, the roof bends and breaks become quicker. As shown in Figure 11 (c2), when the drop is 50 m, the working face only needs to advance 105 m to have the first roof collapses (when the drop is 10 m, the working face advances 140 m when the roof collapses for the first time). After the collapsed rock mass compacts the mined-out area, the damage of the bottom rock mass is suppressed, and

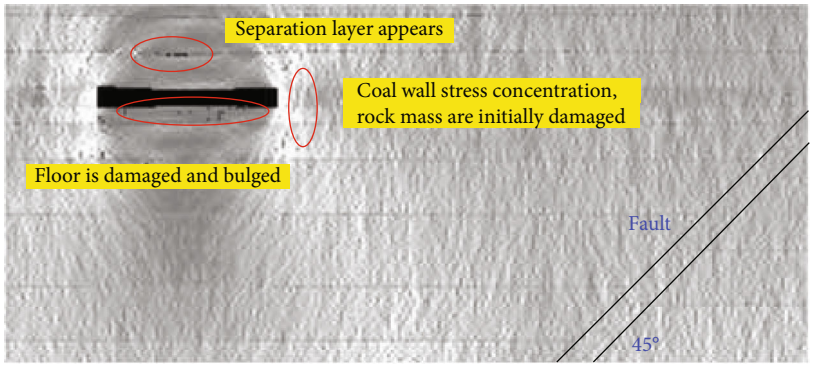

(a) Advancing 50 m of working face

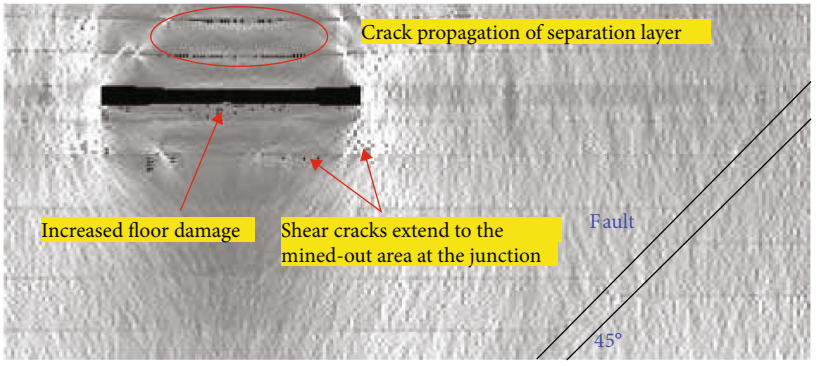

(b) Advancing 75 m of working face

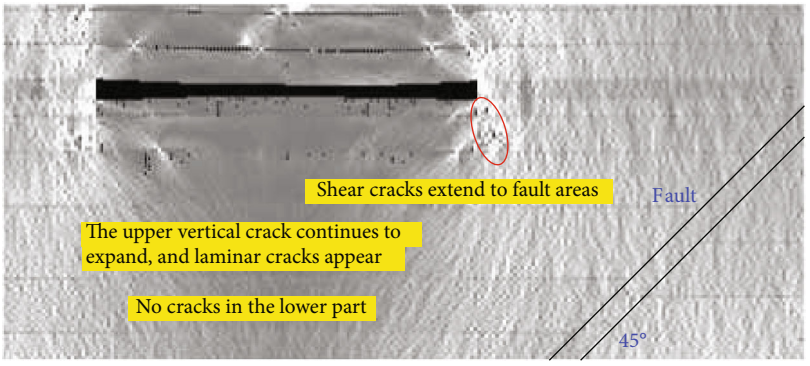

(c) Advancing 105 m of working face

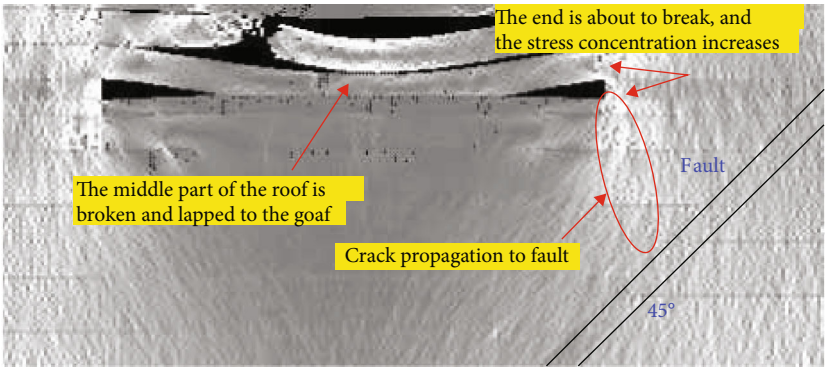

(d) Advancing 140 m of working face

Figure 7: Mining crack evolution process (45°, project 1).

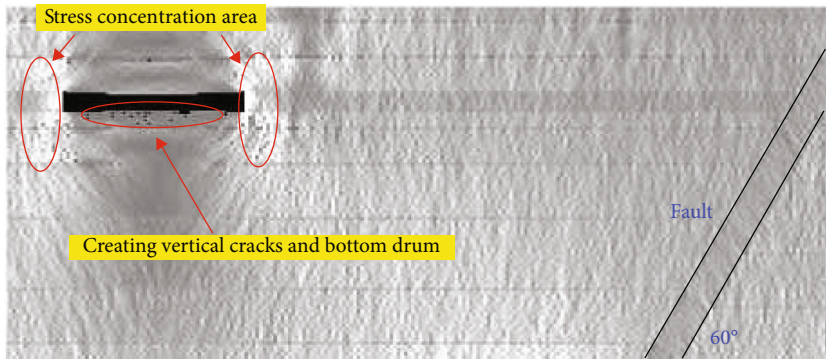

(a) Advancing 50 m of working face

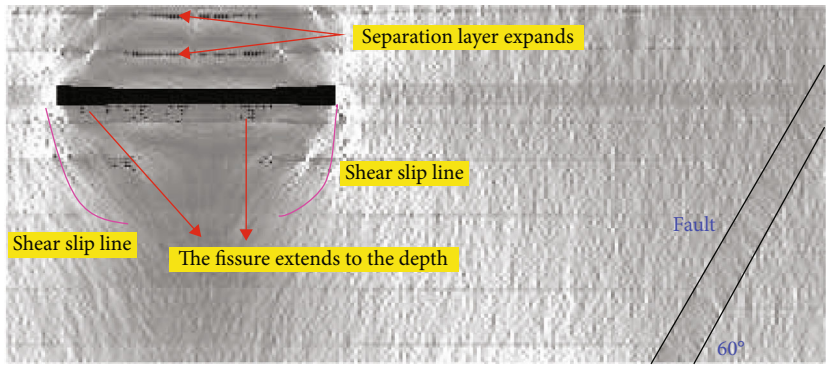

(b) Advancing 75 m of working face

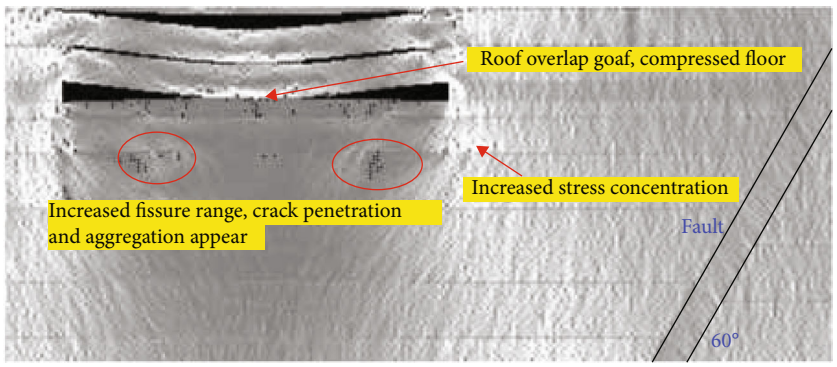

(c) Advancing 105 m of working face

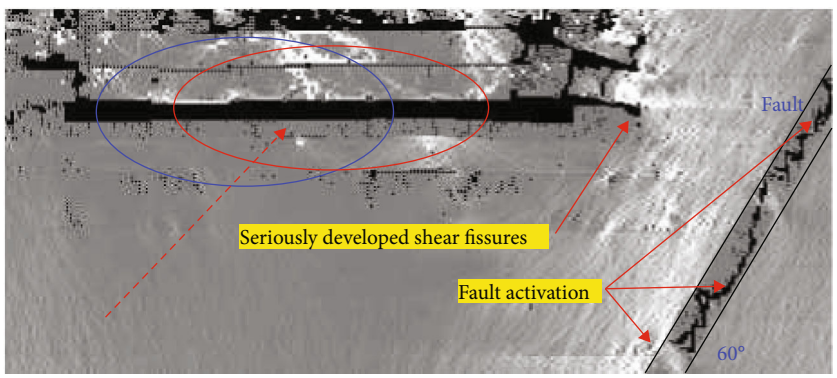

(d) Advancing 140 m of working face

Figure 8: Mining crack evolution process (60°, project 2).

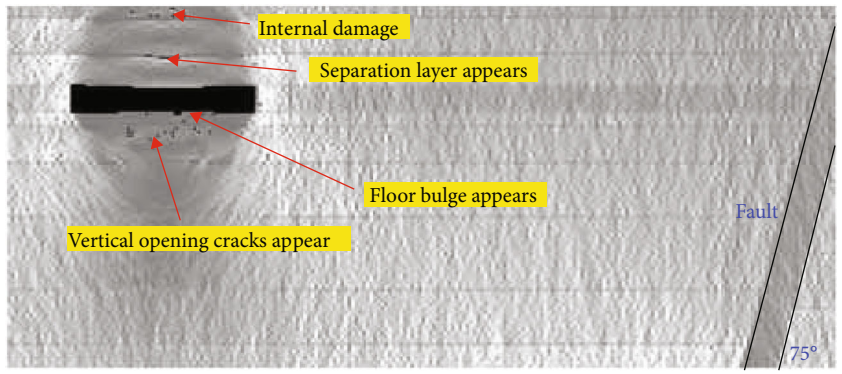

(a) Advancing 50 m of working face

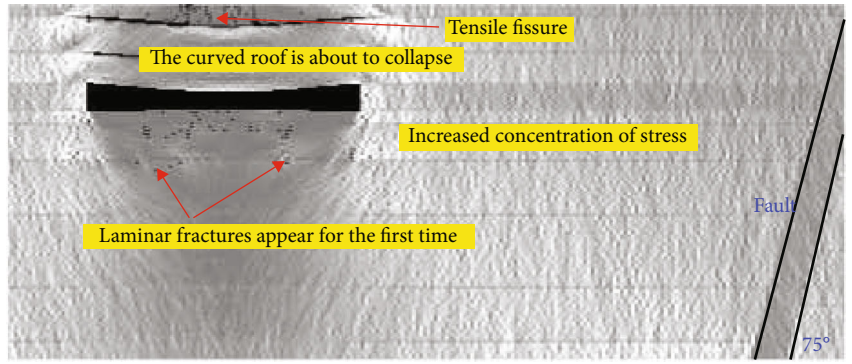

(b) Advancing 75 m of working face

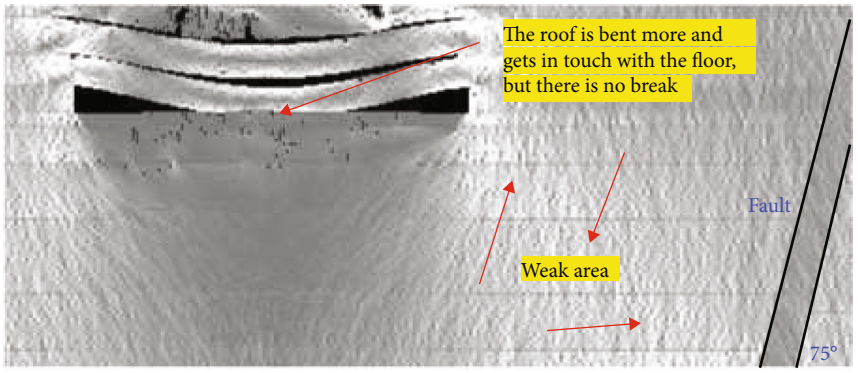

(c) Advancing 105 m of working face

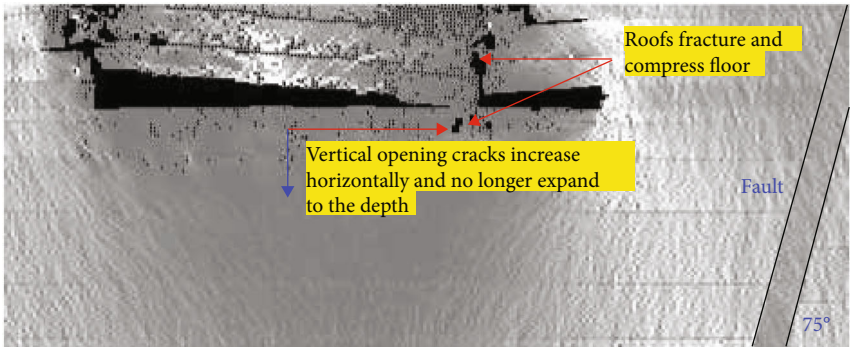

(d) Advancing 140 m of working face

Figure 9: Mining crack evolution process (75°, project 3).

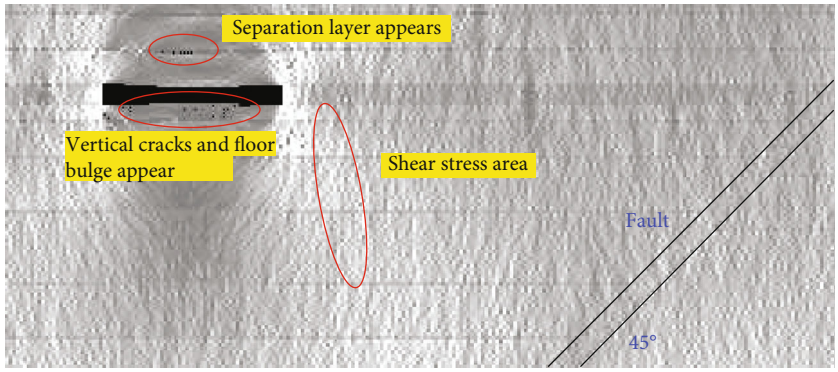

(a) Advancing 30 m of working face

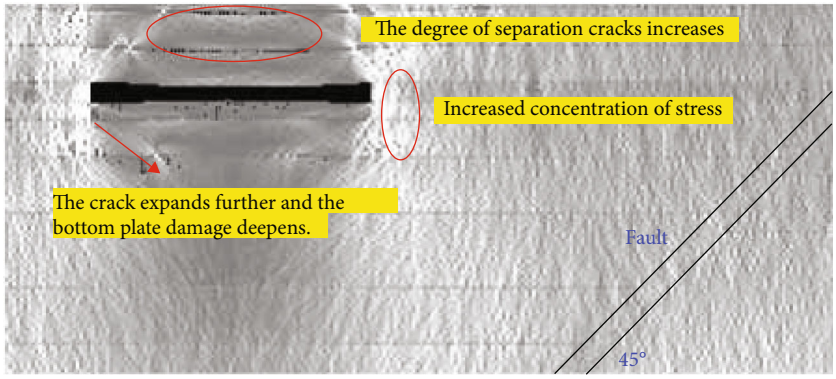

(b) Advancing 75 m of working face

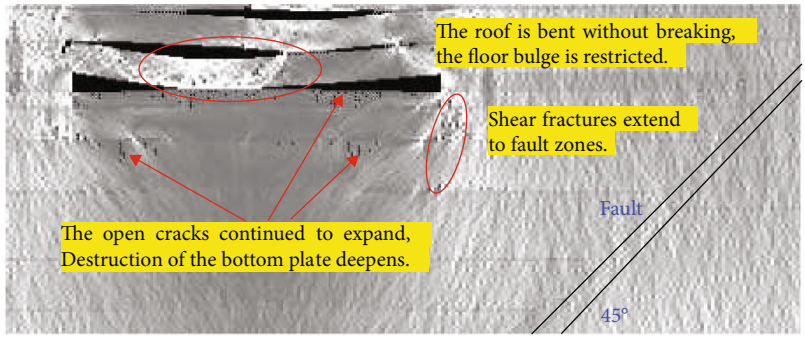

(c) Advancing 105 m of working face

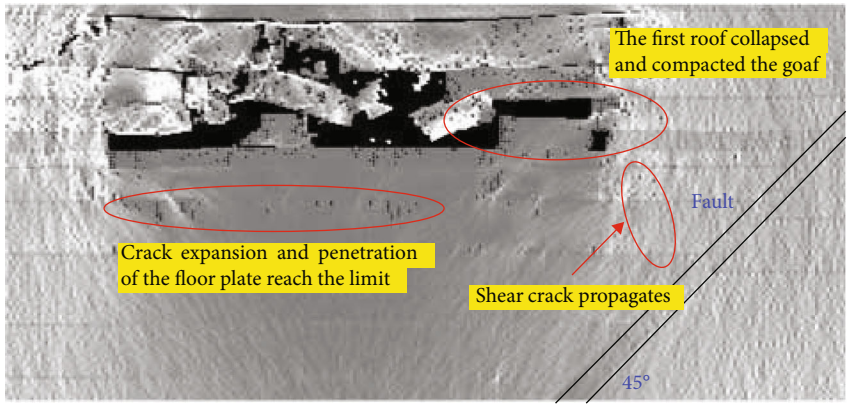

(d) Advancing 140 m of working face

Figure 10: Mining crack evolution process (30 m, project 4).

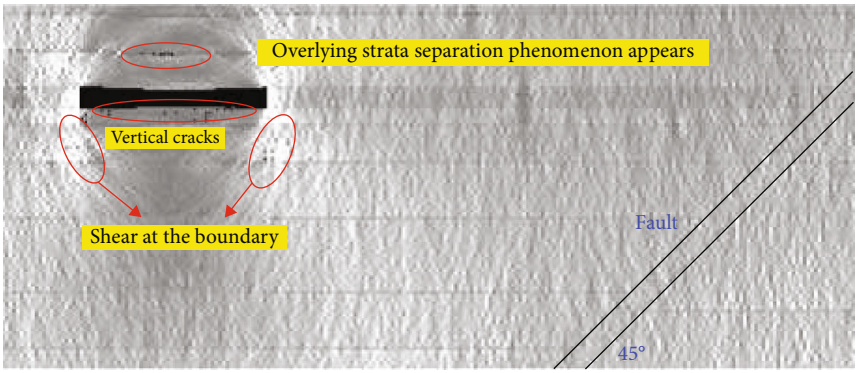

(a) Advancing 30 m of working face

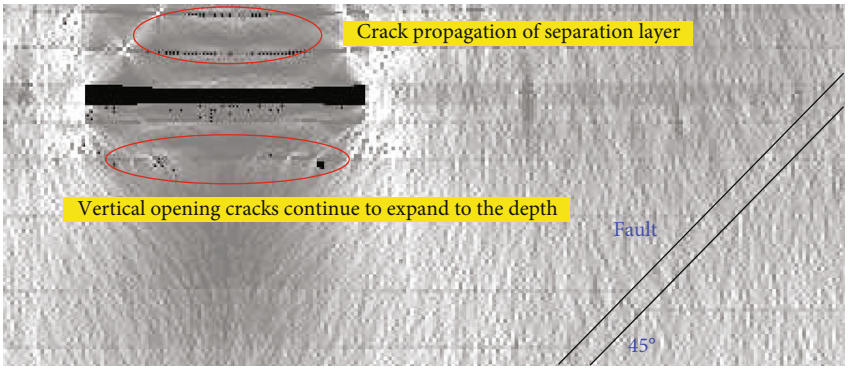

(b) Advancing 75 m of working face

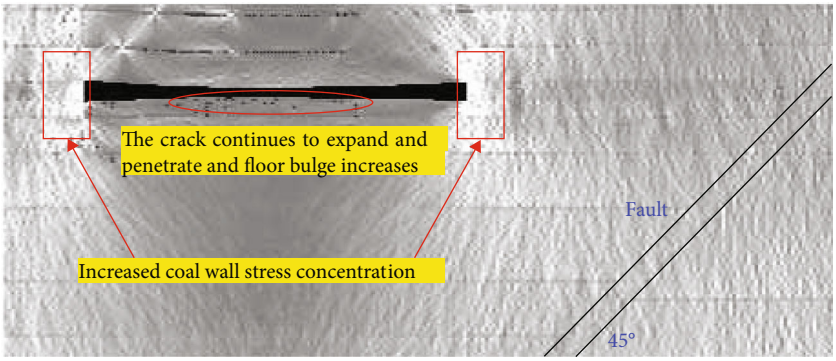

(c) Advancing 105 m of working face

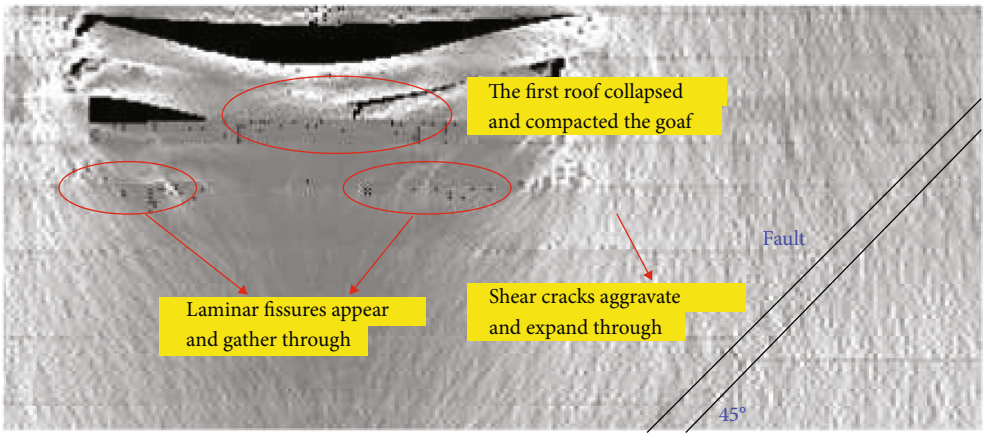

(d) Advancing 140 m of working face

Figure 11: Mining crack evolution process (50 m, project 5).

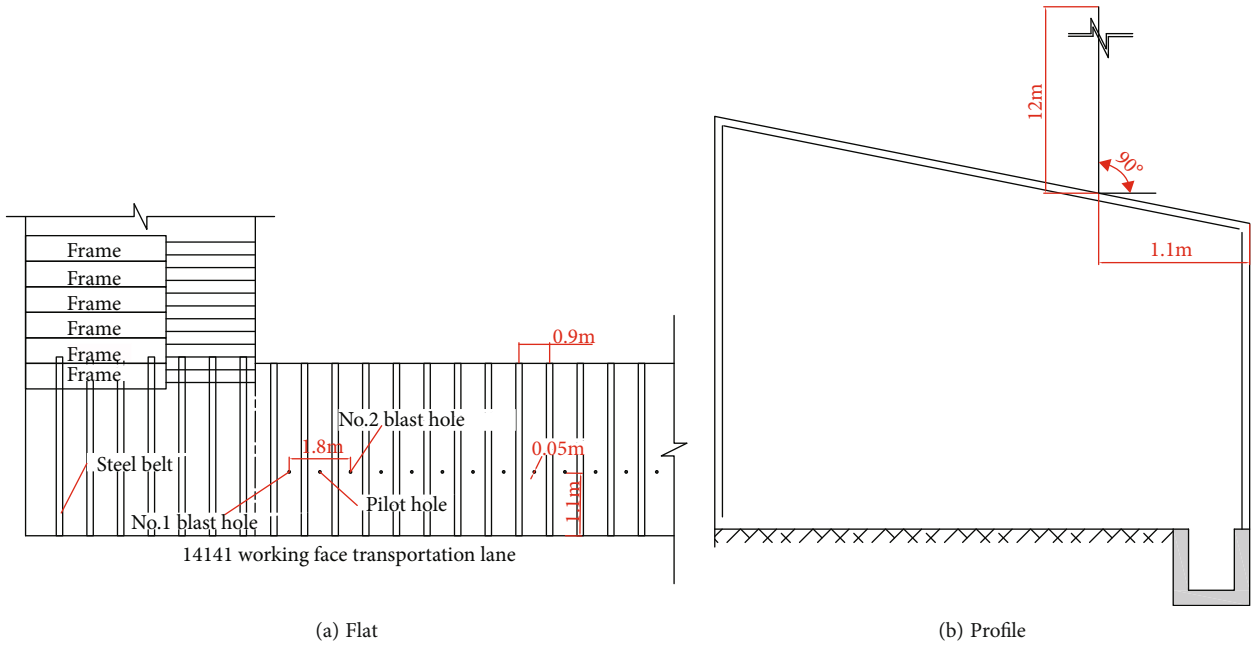

(a) Flat (b) Profile

Figure 12: Arrangement of presplitting blasting holes in transportation lane of 14141 working face.

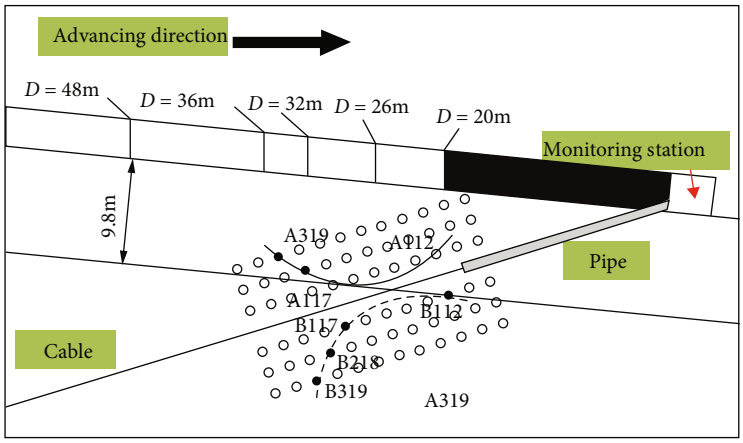

Figure 13: Schematic diagram of floor failure depth.

water inrush disaster will be mitigated afterwards. It is helpful to the prevention for the delayed water inrush in deep buried faults.

The collapse of the roof can effectively restrain the further damage of the seam floor. But whether the damage is aggravated or not during the collapse requires further investigation. Through analysis on Figure 11 (c1 and c2), it can be seen that when the roof collapsed for the first time, no sign of further damage of the seam floor is found but only some increased heaving floor volume. The seam floor propagates and penetrates into the cracks and shear cracks but not into depth. It can also be seen from Figure 11 (c2) that the broken rock mass after the roof collapse exerts pressure on the seam floor, reducing the stress intensity factor of the fault surrounding rock and the cracks of the seam floor rock mass, so that the deformation of the heaving floor weakens. This shows that the roof not only has almost no effect on the seam floor during the process but also mitigating the damage on the seam floor.

The comprehensive analysis shows that the fault drop has little impact on the crack evolution of the floor rock mass with fault but will exert an outstanding impact on the roof failure rate. When the fault drop increases to a certain value, the roof will be broken for the first time during the mining process, restraining the destruction of the seam floor. Therefore, the artificial forced roofing is used on site to effectively reduce the damage of the seam floor. When the real geological conditions have a small fault drop or the roof is difficult to install, artificial forced roofing should be actively adopted. However, it is worth noticing that this article only simulates the fault drop of 10 m, 30 m, and 50 m based on the actual situation. Relationship between time and mechanical of the fault drop and the roof breakage should be further studied.

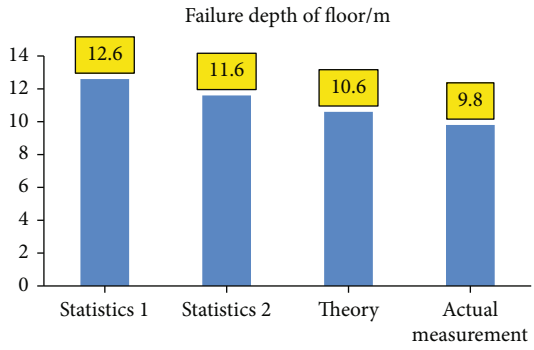

Figure 14: Failure depth of floor.

5. Field Application Analysis

5.1. Mine Overview. The strike length of 14141 working face of Jiulishan Mine of Henan Coking Coal Group is about 748 m, and the slope length is about 111 m. The average thickness of the mined II1 coal seam is 6.9 m, and the average dip angle is 9.5°. The thickness of the L_8 limestone in the floor is about 7.5 m, the water pressure is about 1.5 MPa, and the thickness of the floor water barrier is about 21.5 m. The water inrush coefficient is 0.07 MPa/m, which is bigger than the critical value of water inrush coefficient with tectonic blocks. So it is dangerous to mine normally. In the field, the working face adopts comprehensive mechanized coal mining with inclined stratified long wall, and the roof is treated by all caving methods.

In order to solve the force of the concentrated pressure of the roof on the surrounding rock and floor of the fault after mining in the 14141 working face and to reduce the stress intensity factor of the crack evolution of floor rock mass, an open cut was made at the 14141 working face, and the roof of the transport roadway was precracked with a blasting top cut, as shown in Figure 12. The blasting layout takes references from literature [34].

5.2. Seam Floor Blasting Analysis. Before mining at 14141 working face, evenly distributed special cables are preembedded in the floor borehole, and the floor failure is monitored by the change of apparent resistivity. The monitoring station was set up in the upper transportation gateway about 170 m away from the 14141working face, shown in Figure 13. It can be seen from Figure 13, the solid-line curve is the floor failure boundary contour, and the region of floor failure is above the curve, gradually decreasing from the shallow to deep areas, which conforms to the shape characteristics of inverted saddle. The results indicate that the maximum depth of floor failure is 9.8 m, located in the measuring point A117.

The floor failure depth obtained by statistical and theoretical methods is 12.6 m, 11.6 m, and 10.6 m, respectively, but 9.8 m of actual measurement, shown in Figure 14. It can be seen that the blasting top cut compared to the uncut top causes the seam floor damage depth to decrease by 22.2%, 15.5%, and 7.5%, respectively, indicating that after the blasting and topping of the roof on 14141 working face, the initial pressure and cycle pressure of the working face are significantly shortened. The concentrated stress from the roof to the seam floor also weakens as well as the propagation and penetration of the floor rock mass cracks. This verifies that in theoretical analysis and numerical simulation, by reducing the stress intensity factor of the seam floor rock mass cracks to mitigate the damage on the floor, thus ensuring the safety of coal mining.

6. Conclusions

The paper carried out mechanical analysis on the initiation and propagation of shear cracks, layered cracks, and vertical tension cracks generated by floor rock mass. The initiation and propagation criteria were obtained, and the nature of the rock crack evolution mechanism was revealed. The evolution of floor mining rock mass cracks is mainly related to the stress intensity factors, crack dip angles, and seepage water pressure of type I and type II cracks. The larger the stress intensity factor, the closer the crack dip angle to θ_0, the easier for cracks to propagate.

The sequence of the formation of cracks in deep floor rock mass with fault is vertical tension cracks, shear cracks, and layered cracks. The locations of the three types of cracks are different. The initiation and propagation of the shear cracks in the coal wall promote the activation of the fault, whereas the vertical tension cracks and the layered cracks have almost no impact on the activation of the faults.

There is at least one certain value between the inclination of the fault between 45° and 75°, which makes the activation degree of the fault reach the maximum; the fault drop has no obvious impact on the crack evolution of the floor mining rock mass and will not cause the activation of the fault and the increase of the drop. Increasing drop causes roof's first collapses in advance, reducing the possibility of water inrush before that and can effectively lower down the risk of continuous damage and water inrush disaster.

Data Availability

Data are obtained from the experiment.

Conflicts of Interest

The authors declare that they have no conflicts of interest.

References

[1] L. SHI and R. N. SINGH, "Study of mine water inrush from floor strata through faults," *Mine Water and the Environment*, vol. 20, no. 3, pp. 140–147, 2001.

[2] S. LIU, W. LIU, and D. YIN, "Numerical simulation of the lagging water inrush process from insidious fault in coal seam floor," *Geotech Geological Engineering*, vol. 35, no. 3, pp. 1013–1021, 2017.

[3] H. Herrmann and H. Bucksch, Eds., "Underground water inrush," in *Dictionary Geotechnical Engineering/Wörterbuch Geo Technik: English-German/Englisch-Deutsch*, Springer Berlin Heidelberg, Berlin, Heidelberg, 2014.

[4] Q. ZHOU, J. HERRERA, and A. HIDALGO, "The numerical analysis of fault-induced mine water inrush using the extended finite element method and fracture mechanics," *Mine Water and the Environment*, vol. 37, no. 1, pp. 185–195, 2018.

[5] D. MA, J. X. ZHANG, H. Y. DUAN et al., "Reutilization of gangue wastes in underground backfilling mining: overburden aquifer protection," *Chemosphere*, vol. 264, p. 128400, 2021.

[6] L. LI, C. TANG, and Z. LIANG, "Numerical analysis of pathway formation of groundwater inrush from faults in coal seam floor," *Chinese Journal of Rock Mechanics and Engineering*, vol. 28, no. 2, pp. 290–297, 2009.

[7] C. QIU, *Rock Concrete Fracture Mechanics*, Wuhan University of Technology Press, 1991.

[8] J. CHEN, Q. WU, and L. YIN, "Law of crack evolution in floor rock mass above high confined water," *Coal Science and Technology*, vol. 46, no. 7, pp. 54–60, 2018.

[9] P. Hou, F. Gao, Y. Ju, Y. Yang, Y. Gao, and J. Liu, "Effect of water and nitrogen fracturing fluids on initiation and extension of fracture in hydraulic fracturing of porous rock," *Journal of Natural Gas Science and Engineering*, vol. 45, pp. 38–52, 2017.

[10] S. WANG, L. SUN, X. LI et al., "Experimental investigation of cuttability improvement for hard rock fragmentation using conical cutter," *International Journal of Geomechanics*, vol. 21, no. 2, article 06020039, 2021.

[11] J. Chen, J. Zhao, S. Zhang, Y. Zhang, F. Yang, and M. Li, "An experimental and analytical research on the evolution of mining cracks in deep floor rock mass," *Pure and Applied Geophysics*, vol. 177, no. 11, pp. 5325–5348, 2020.

[12] Q. Zhang, Q. Jiang, X. Zhang, and D. Wang, "Model test on development characteristics and displacement variation of water and mud inrush on tunnel in fault fracture zone," *Natural Hazards*, vol. 99, no. 1, pp. 467–492, 2019.

[13] L. YIN and J. CHEN, "Experimental study of influence of seepage pressure on joint stress-seepage coupling characteristics," *Rock and Soil Mechanics*, vol. 34, no. 9, pp. 2563–2568, 2013.

[14] J. CHEN, W. GUO, and L. YIN, "Experimental study of floor cracking under deep mining," *Chinese Journal of Rock Mechanics and Engineering*, vol. 35, no. 11, pp. 2298–2306, 2016.

[15] S. WANG, X. LI, J. YAO et al., "Experimental investigation of rock breakage by a conical pick and its application to non-explosive mechanized mining in deep hard rock," *International Journal of Rock Mechanics and Mining Sciences*, vol. 122, p. 104063, 2019.

[16] S. Zhang, W. Guo, Y. Li, W. Sun, and D. Yin, "Experimental simulation of fault water inrush channel evolution in a coal mine floor," *Mine Water and the Environment*, vol. 36, no. 3, pp. 443–451, 2017.

[17] Y. GUO, Y. ZHAO, S. WANG, G. FENG, Y. ZHANG, and H. RAN, "Stress-strain-acoustic responses in failure process of coal rock with different height to diameter ratios under uniaxial compression," *Journal of Central South University*, vol. 28, no. 6, pp. 1724–1736, 2021.

[18] D. Ma, S. B. Kong, Z. H. Li, Q. Zhang, Z. H. Wang, and Z. L. Zhou, "Effect of wetting-drying cycle on hydraulic and mechanical properties of cemented paste backfill of the recycled solid wastes," *Chemosphere*, vol. 282, p. 131163, 2021.

[19] Q. Wu, X. Guo, J. Shen, S. Xu, S. Liu, and Y. Zeng, "Risk assessment of water inrush from aquifers underlying the Gushuyuan coal mine, China," *Mine Water and the Environment*, vol. 36, no. 1, pp. 96–103, 2017.

[20] J. HE, W. LI, and W. QIAO, "P-H-qevaluation system for risk assessment of water inrush in underground mining in North China coal field, based on rock-breaking theory and water-pressure transmission theory," *Geomatics Natural Hazards & Risk*, vol. 9, no. 1, pp. 524–543, 2018.

[21] W. SUN and Y. XUE, "An improved fuzzy comprehensive evaluation system and application for risk assessment of floor water inrush in deep mining," *Geotechnical and Geological Engineering*, vol. 36, no. 6, pp. 1–11, 2018.

[22] H. Yin, H. Zhao, D. Xie, S. Sang, Y. Shi, and M. Tian, "Mechanism of mine water inrush from overlying porous aquifer in quaternary: a case study in Xinhe Coal Mine of Shandong Province, China," *Arabian Journal of Geosciences*, vol. 12, no. 5, 2019.

[23] W. Guo, J. Zhao, L. Yin, and D. Kong, "Simulating research on pressure distribution of floor pore water based on fluid-solid coupling," *Arabian Journal of Geosciences*, vol. 10, no. 1, pp. 1–14, 2017.

[24] N. ERARSLAN, Z. LIANG, and D. WILLIAMS, "Experimental and numerical studies on determination of indirect tensile strength of rocks," *Rock Mechanics and Rock Engineering*, vol. 45, no. 5, pp. 739–751, 2011.

[25] J. CHEN, *Basic Experimental Research of Floor Cracking and Crack Propagation in Deep Mining*, Shandong University of Science and Technology, Qingdao, 2014.

[26] W. SUN, Y. XUE, and L. YIN, "Experimental study on seepage characteristics of large size rock specimens under three-dimensional stress," *Geomechanics and Engineering*, vol. 18, no. 6, pp. 567–574, 2019.

[27] D. MA, J. J. WANG, X. CAI et al., "Effects of height/diameter ratio on failure and damage properties of granite under coupled bending and splitting deformation," *Engineering Fracture Mechanics*, vol. 220, p. 106640, 2019.

[28] X. Wang, T. Wang, Q. Wang, X. Liu, R. Li, and B. J. Liu, "Evaluation of floor water inrush based on fractal theory and an improved analytic hierarchy process," *Mine Water and the Environment*, vol. 36, no. 1, pp. 87–95, 2017.

[29] Y. Zhao, Q. Peng, W. Wan, W. Wang, and B. Chen, "Fluid-solid coupling analysis of rock pillar stability for concealed karst cave ahead of a roadway based on catastrophic theory," *International Journal of Mining Science and Technology*, vol. 24, no. 6, pp. 737–745, 2014.

[30] W. Li, Y. Liu, X. Yao, J. Chu, X. Chen, and Z. Tan, "Study on breakdown pressure in hydraulic fracturing process of hard rock based on numerical simulation," *Geotechnical and Geological Engineering*, vol. 39, no. 2, pp. 909–917, 2021.

[31] J. SUN, Y. HU, and G. ZHAO, "Relationship between water inrush from coal seam floors and main roof weighting," *International Journal of Mining Science and Technology*, vol. 27, no. 5, pp. 873–881, 2017.

[32] H. Lu, D. Yao, D. Shen, and J. Cao, "Fracture mechanics solution of confined water progressive intrusion height of mining fracture floor," *International Journal of Mining Science and Technology*, vol. 25, no. 1, pp. 99–106, 2015.

[33] D. LIU, H. SUN, and Y. ZHANG, "A model of shear slipping of overlying strata under mining disturbance," *Rock and Soil Mechanics*, vol. 31, no. 2, pp. 609–614, 2010.

[34] Y. XU, Y. LUO, and S. ZHANG, "Practical study of mining failure of working face floor with roof cutting pressure relief," *Coal Mining Technology*, vol. 23, no. 6, pp. 94–98, 2018.